UNCLASSIFIED

AD NUMBER
AD411166
LIMITATION CHANGES
TO: **Approved for public release; distribution is unlimited.**
FROM: **Distribution authorized to U.S. Gov't. agencies and their contractors; Administrative/Operational Use; 01 APR 1963. Other requests shall be referred to Office of Naval Research, Arlington, VA 22203.**
AUTHORITY
ONR ltr dtd 4 May 1977

THIS PAGE IS UNCLASSIFIED

(5) 853 100

TYCO LABORATORIES, INC.
BEAR HILL, WALTHAM 54, MASSACHUSETTS
AREA CODE 617
TELEPHONE: 899-1650

(1)

ELECTROCHEMISTRY OF FUEL CELL ELECTRODES

Kinetics of Redox Reactions on Passive Electrodes

by

A. C. Makrides
Principal Investigator

Technical Memorandum No. 2

Contract No. Nonr-3765(00)
dated April 16, 1962
expiring April 15, 1963

ARPA Order ~~No.~~ 302-62
~~Project Code~~ 9800
Task ~~No.~~ NR 359-443

April 1, 1963
prepared for:
OFFICE OF NAVAL RESEARCH
Materials Sciences Division
Washington 25, D.C.

ABSTRACT

Polarization measurements for the $Fe^{(+++)}/Fe^{(++)}$ couple on passive Ni, Fe, and Ti were carried out in solutions of fixed ionic strength but of varying pH. Tafel lines were generally obtained with exchange currents 10^{-7} ~~to 10^{-5}~~ amp/~~cm^2~~ sq cm and cathodic transfer coefficients about 0.45. The anodic transfer coefficients were less, particularly with Ti and Fe electrodes. A limiting anodic current, which was unrealted to diffusion of $Fe^{(++)}$ ion in solution, was observed under certain conditions on passive Fe and Ti.

The contribution of ionic current to the total current trhough the film is negligible in most cases . In general, the passive film has rectifying properties, i.e., the easy direction of electron flow is from metal to solution. This rectification is additional to the usual Faradaic rectification observed with most electrochemical reactions. The apparent transfer coefficients, calculated from the anodic and cathodic polarization curves, yield sums significantly less than unity. The results suggest that a potential drop exists across the surface film, that it depends on the thickness and composition of the film, and that it has a substantial effect on the electrode kinetics of $Fe^{(++)}$ oxidation on passive electrodes.

* 10 to the -7th power to 10 to the -5th power

Introduction

The formation of a surface oxide is an important factor in the kinetics of oxygen evolution and oxygen reduction on practically all metallic electrodes(1). In general, a superficial oxide is expected to change the specific interaction of oxygen (or of reaction intermediates) with the electrode, to alter the potential distribution between metal and electrolyte, and to modify the dissolution kinetics of the metal. The change in the kinetics of dissolution has been studied in detail since it is the characteristic phenomenon in passivity(2-6). However, relatively little work has been done on the effects of oxide films on electrochemical reactions other than corrosion reactions. The general features of electrode processes on superficially oxidized metals are examined in this paper using as a model a simple, one-electron redox reaction.

Aside from specific effects, e.g., changes in the energy of adsorption of reactants or of intermediates, superficial oxides may influence the kinetics of an electrochemical reaction by providing a barrier to electron transfer between the metal and an ion or molecule at the oxide/electrolyte interface. With thick films, the oxide is the electrode, the underlying metal serving merely as a contact. The chemical character of the bulk oxide and its electrical properties, e.g., its semiconducting properties, enter then into the description of its electrode characteristics. At the other extreme, very thin oxide films may be considered as simply providing a barrier through which electrons must tunnel in order to participate in the reaction. The upper limit for tunneling is about 30 A; conduction through the oxide is necessary for electron transfer with thicker films. However, if the film is only 100-200 A, its electrical characteristics are influenced strongly by the underlying metal. This interaction may be important in the description of the electrode behavior of superficially oxidized electrodes.

A simple way of examining the general electrochemical effects of surface oxides is to compare the kinetics of an elementary electron transfer reaction on oxide-covered and oxide-free electrodes. Specific effects, e.g., adsorption, should be at a minimum for the redox couple chosen. The Fe^{+++}/Fe^{++} couple was selected in this study because its kinetic behavior on oxide-free electrodes is straightforward(7, 8). Furthermore, since its reversible potential falls in about the middle of the potential region over which a number of common metals and alloys are passive, both the oxidation of ferrous ion and the reduction of ferric ion can be followed without gross interference from corrosion reactions.

Experimental

The electrochemical cell was described previously(9). Potentials were measured through a Luggin-Haber capillary probe 0.05 cm O.D. placed 0.10 cm from the electrode surface. The iR drop between electrode and capillary probe was negligible at all currents. A high impedence circuit (residual current less than 10^{-12} amp) was used in measuring potentials. Constant current was drawn from high capacity batteries through variable resistances. The cell was thermostated to within ±0.05°C.

The cell and its attachments were cleaned in concentrated chromic + sulfuric acid solution (cleaning solution). Ground-glass joints were of the cup type and were sealed with water. The solution around the electrode was stirred with argon which had been passed over copper at 500°C and through a cold trap (dry ice-acetone). Laboratory distilled water was distilled from dilute $KMnO_4$ into a two-stage, quartz still and from there into quartz storage flasks. Reagents were of C.P. grade. A series of experiments with twice-recrystallized ferrous and ferric salts showed no significant differences from experiments with C.P. reagents.

Electrodes were rods or spheres about 1 cm^2 in projected area. They were mounted on assemblies in which only glass and Teflon, besides the electrode, came in contact with solution(10). The electrodes were cleaned in cleaning solution followed by rinsing with boiling, triply distilled water. The passive film was formed in the solution after cathodic treatment of the electrode. Nickel and titanium passivated spontaneously in the ferric solutions.

Exploratory studies showed that the current densities at which appreciable polarization is observed with all of the above electrodes (when passive) were substantially less than the expected diffusion-limited currents for both Fe^{+++} and Fe^{++} ions. An estimate of the diffusion-limited current density, i_d, can be made from:

$$i_d = nFkc = nF \frac{D}{\delta} c \qquad (1)$$

where the heterogeneous rate constant, k, is given by the ratio of the diffusion constant, D, to the effective thickness, δ, of the boundary layer for diffusion. Although neither D nor δ are known precisely, good estimates for both quantities are available. A conservative estimate of D is 5×10^{-6} cm^2/sec(11); δ is about 5×10^{-3} cm for stirring by gas(12). The diffusion rate constant is then 1×10^{-3} cm/sec and the diffucion-limited current at c = 0.05 M/l is $5. 10^{-3}$ amp/cm^2. The maximum applied current density was substantially less than this, except in the case of nickel. With other than nickel electrodes, direct proof of the absence of concentration polarization was provided by the insensitivity of the measured potential to stirring. On nickel electrodes there was a difference of about 15 mv between the potential measured in stagnant and in stirred solutions at a current density of 10^{-3} amp/cm^2. We estimate the concentration overpotential in stirred solutions at 10^{-3} amp/cm^2 to be less than 5 mv.

Discussion

The overpotential parameters derived from the polarization curves of Figs. 1-3 are given in Table I. Noteworthy features are the low exchange currents, the unusual values of the transfer coefficients, and the pronounced assymetry of the anodic and cathodic reactions on iron and titanium. These characteristics may be contrasted with results on Pt electrodes in M H_2SO_4(7). The exchange current on Pt with $C_{Fe^{+++}} = C_{Fe^{++}} = 0.05$ M/l is 1.5×10^{-2} amp/cm^2; the anodic transfer coefficient is 0.58 ± 0.02 and the cathodic transfer coefficient 0.42 ± 0.02(7). It should be noted that experiments in M H_2SO_4 without salt show that $MgSO_4$, the inert electrolyte used for keeping the composition of the double layer essentially constant, does not participate in the reaction nor does it have any major effect on the kinetics.

Previous work with redox reactions on superficially oxidized electrodes has been concerned mainly with the kinetics of redox reactions on stainless steel$^{(13-15)}$ where redox couples can be used to inhibit dissolution. Redox reactions on passive stainless steel have been discussed in a conventional way $^{(14)}$, although they exhibit features similar to those noted here, i.e., extremely small exchange currents and unusual values of transfer coefficients with sums generally less than unity$^{(13)}$.

Meyer$^{(16)}$ studied a number of cathodic reactions on anodically oxidized zirconium electrodes. He showed that the unusual transfer coefficients and reaction orders which he observed can arise from a dual energy barrier and suggested a model in which the reaction rate depends both on the potential drop across the oxide and across the electrolytic double layer. The present results also suggest that a significant potential drop across the surface oxide exists and that it is important in determining the overall reaction rate. However, the dual barrier model as formulated originally$^{(16)}$ does not entirely fit the present results. It is assumed in this model that two potential-dependent processes occur, one corresponding to a film reaction and the other to a double layer reaction. Their rates are given by:

$$i_c = i_{o,f} \exp(-\alpha_f V_f) \tag{2a}$$

and

$$i_c = i_{o,e} \exp(-\alpha_r V_r) \tag{2b}$$

where the potentials are in units of RT/F, and where:

$$E = V_f + V_r \tag{3}$$

The apparent cathodic transfer coefficient is:

$$\alpha_c = \left(\frac{\partial \ln i_c}{\partial E}\right)_T = -\frac{\alpha_f \alpha_r}{\alpha_f + \alpha_r} \tag{4}$$

Similarly, the apparent anodic transfer coefficient is:

$$\alpha_a = \left(\frac{\partial \ln i_a}{\partial E}\right)_T = \frac{\beta_f \beta_r}{\beta_f + \beta_r} \tag{5}$$

where

$$\alpha_f + \beta_f = 1 \qquad \text{and} \qquad \alpha_r + \beta_r = 1 \tag{6}$$

From Equations (4-6) and the experimentally determined anodic and cathodic apparent transfer coefficients we can calculate α_f and α_r (or β_f and β_r). The values so calculated are not reasonable. This can be demonstrated easily if we assume $\alpha_r = \beta_r \simeq 0.5$. If then $\alpha_f \simeq 0.5$, the apparent anodic and cathodic coefficients should be ~ 0.25 with a sum of 0.5. These values do not correspond with what is observed generally. If, on the other hand, we choose α_f so as to make the apparent cathodic coefficient reasonably close to what is observed, then the anodic coefficient calculated from Eq. (6) is unreasonable. For example, assuming again $\alpha_r = \beta_r \simeq 0.5$ and taking $\alpha_f = 0.90$, the apparent cathodic coefficient, $\alpha_c = 0.32$, is not far from what is found on most electrodes. However, the calculated apparent anodic transfer coefficient is now only 0.08, which is substantially less than observed. In general, fractional values of α_f and β_f do not lead to the experimentally observed apparent transfer coefficients assuming for α_r and β_r either 0.5, or the values found on Pt.

The Redox Reaction. In interpreting the results presented here, we note that all molecular processes for the Fe^{+++}/Fe^{++} reaction occur on the aqueous side of the interface and that the electrode serves only as a reservoir of electrons at a fixed electrochemical potential. We expect in a first approximation that the exchange current and the transfer coefficients on oxide-free, inert electrodes, e.g., Pt or Hg, are characteristic of the couple(17-19). If the surface layer on oxidized electrodes modifies electron transfer between electrode and solution in a major way, substantial changes in the redox kinetics may occur. It is assumed in the following discussion that the redox reaction proper occurs in a normal fashion and that differences of characteristic kinetic parameters between passive and metallic electrodes are due to the electron transfer process through the superficial film.

The fundamental concepts of electron exchange between a metal and a redox couple in solution developed by Gurney(17) were recently reformulated and extended to semiconductors by Gerischer(19). The basic postulate of the theory is that a weak electronic interaction occurs between the ion and the electrode(18); consequently, electron exchange is adiabatic, i.e., it occurs between the same energy levels in the two phases. Gerischer(19) introduced the concept of electron energy states in a redox electrolyte in analogy to the notion of energy levels in a solid. For example, the energy of unoccupied states is defined by the energy change accompanying the introduction of an electron from infinity to the lowest state of an oxidized ion without changing its solvation structure. It can be shown that the equilibrium distribution of available energy levels follows a Fermi distribution function where the "Fermi" level of the electrolyte is directly related to the mean free energy change accompanying the redox reaction.

The current flowing from electrode to electrolyte is given by(19):

$$i_c = e_o \int_{-\infty}^{+\infty} P(\epsilon) \cdot D_{el}(\epsilon) \cdot f(\epsilon - \epsilon_{f,el}) \cdot D_{redox}(\epsilon) \cdot f(\epsilon_{f,\,redox} - \epsilon)\, d\epsilon \qquad (7)$$

Here, e_o is the electronic charge, D_{el} and D_{redox} the density of states function for the electrode and electrolyte respectively, and $f(\epsilon - \epsilon_{f,el})$ and $f(\epsilon_{f,\,redox} - \epsilon)$ the Fermi distribution functions for the two phases. $P(\epsilon)$ is a proportionality factor which contains the frequency with which electrons arrive at the electrode/electrolyte boundary and the tunneling probability through the potential barrier between the two phases.

The exchange current, i_c at $\eta = 0$ for semiconductors can be drastically smaller than for metal electrodes, since the actual density of states near the Fermi level where most of the exchange takes place on metal electrodes, may be very small for a semiconductor. Thus, a main result of the theory is that the exchange current on semiconductor electrodes may be smaller than on metals by orders of magnitude.

The small exchange currents found for the Fe^{+++}/Fe^{++} reaction on passive electrodes can be viewed as a consequence of a decrease of $P(\epsilon)$. This may be due either to a substantial decrease in the tunneling probability or to the semiconducting character of the superficial film. It is shown below that the current changes by only a small factor (<10) when the film thickness changes by a factor of about 2. This rules out a rate limiting process involving electron tunneling across the oxide. It is probable that the small exchange currents (Table I) are a consequence of the semiconductor characteristics of the passive film.

Rectification. For most redox reactions, the i-E characteristics are not entirely symmetrical on anodic and cathodic polarization, the effect being attributable to Faradaic rectification. The rectification ratio is small generally; for example, the Fe^{+++}/Fe^{++} reaction on Pt exhibits anodic and cathodic transfer coefficients of 0.58 and 0.42 (Table II), so that the corresponding currents at $\eta = 100$ mv are in the ratio of 1/0.55. A considerably more pronounced rectification in the opposite direction is observed with passive electrodes (e.g. Fe and Ti, Table II). In general, the transfer coefficient for Fe^{+++} reduction on passive electrodes is close to the value found on platinum. However, the anodic transfer coefficients are invariably smaller, frequently by a substantial amount.

Rectification by anodically formed surface oxides is well-known for valve metals (Ta, Zr, etc.)(20-23). The direction of easy electron flow is from metal to electrolyte. The magnitude of the current depends in a complicated way on the conditions of formation of the oxide and on surface preparation. The current can be increased by cathodic "deformation" but is restored to its previous value by subsequent anodic polarization(23).

A number of possible mechanisms for rectification by anodic oxide films have been advanced(21-25). Vermilyea(25) demonstrated the existence of weak spots in oxide films on valve metals and showed that most of the cathode current flows through these imperfections. Although rectification was attributed to areas of defective oxide, no mechanism for the rectifying properties, as contrasted to its higher conductivity, was suggested for the defective oxide(25). The most likely explanation of rectification, which applies either to the film as a whole, or to weak or thin spots in the film, is that due to van Geel who postulates a p-n junction with the oxide(23, 24).

The rectification observed with passive films, is similar in some respects to that observed with oxides on valve metals. However, the thinness of the passive film makes it unlikely that the continuum description implied by the term "semiconductor" is applicable. It is preferable to adopt a chemical approach to the description of the electrical characteristics of the film, as was done by Vetter(26) and more recently by Nagyama and Cohen(27). The latter authors suggest that the passive film in the case of Fe consists of an inner layer approaching Fe_3O_4 and an outer layer of "γ-Fe_2O_3" with a defect structure of the form $Fe^{+6}_{x}\ Fe^{+3}_{2-2x}\ \square_{x}\ O_3$. Although a film of this sort may be described as a "semiconductor", it could not possibly support a space-charge region which is what basically gives rise to the rectifying properties of semiconductors.

Rectification by passive electrodes is probably caused by the distribution of the total potential from metal to solution between the film and the oxide/electrolyte interface. The potential drop across the passive film appears to be a constant fraction of the total applied potential. Therefore, the overpotential for oxidation of Fe^{++} is $(1 - \gamma)\eta$, and the apparent transfer coefficient for the anodic reaction is $(1 - \gamma)\beta_r$, where γ is the fraction of the total potential which is across the film. This argument is developed in more detail in a subsequent communcation dealing with the kinetics of the Fe^{+++}/Fe^{++} reaction on passive Fe-Cr alloys (Technical Memorandum No. 4).

Ionic and Electron Currents. Both an ionic current and an electronic current may flow through a passive electrode at any potential. The steady-state ionic current, which may be observed in the absence of the redox couple, is generally a small fraction of the total current plotted in Figures 1 - 3. For example, the steady-state corrosion current (equivalent to the ionic current) for Ti is less than 10^{-7} amp/cm^2 and is independent of the potential in the passive region. The total current with a redox couple in solution depends, of course, on the potential and can be as much as 10^{-3}

amp/cm^2. In the discussion above it was assumed that all the current which flows when a redox couple is added to the solution is electronic.

Although the ionic process does not contribute significantly to the observed current (however, see the case of Fe below), it may still have a substantial effect on the total i-E characteristics either because of changes in film thickness with potential or because of changes in film composition, particularly on anodic polarization. The commonly accepted account of the kinetics of growth and of dissolution of passive films is due to Vetter(26). Oxide growth is assumed to be by field-assisted migration of cations through the film. Contrary to the case of oxides on valve metals, the passive film dissolves in common electrolytes at an appreciable rate. The dissolution process is a purely chemical reaction with a rate independent of potential. In the steady state, the rate of film growth equals its dissolution rate at some (stationary) oxide thickness. If the potential is changed to a more positive value, oxide formation at the higher field is initially faster than dissolution. As the film grows, the field across it is reduced until the formation and dissolution rates again balance each other. This mechanism accounts for the most notable characteristic of passive electrodes, namely, a steady-state, anodic oxidation current which is independent of potential.

Consider an electrode on which the film has grown to its steady-state thickness corresponding to the reversible Fe^{+++}/Fe^{++} potential. If the electrode is polarized anodically, an ionic and an electronic current flow across the film. The ionic current is originally larger than its steady-state value since the potential gradient across the film is increased. The ionic current decreases as the film thickens and approaches eventually its former value which is of the order of 10^{-7} a/cm^2 for Ti and 10^{-6} a/cm^2 for Ni. The oxide thickness must, therefore, increase continuously with potential on anodic polarization. On the other hand, the oxide thickness may not change appreciably from its value at the reversible potential upon cathodic polarization if the dissolution rate is 10^{-6} a/cm^2 or less, and if substantial electrochemical reduction of the film does not occur in the potential range in question. This can easily be seen when the dissolution rate is translated into film equivalents. At 10^{-6} a/cm^2, about

15 min would be required to remove about 10 A of film ($\sim 10^{-3}$ coul/cm^2), or approximately a unit cell of oxide. Thus, it is probable that the film thickness on passive Ni or Ti does not change in the course of a cathodic run. However, the dissolution rate is substantially higher (10^{-5} a/cm^2) in the case of iron so that significant changes in film thickness must occur during cathodic polarization also.

Nickel Electrodes. The Fe^{+++}/Fe^{++} reaction on nickel electrodes was examined at various pH and temperatures. Since films of varying stationary thickness are produced at different pH, it is possible to observe changes (if any) in the redox kinetics with oxide thickness. Results are given in Table II and Figs. 4 - 6.

The exchange current increases with decreasing pH. It approximately doubles between pH of 2.3 and 0.0. The cathodic transfer coefficient increases from 0.41 to 0.47 over the same pH range. Therefore, the total cathodic current at any given overpotential increases by a factor of slightly greater than 2 in this acidity range.

Fig. 4 shows that the anodic polarization curve changes in a substantial way when the pH decreases. The total anodic current at overpotentials between -0.050 and +0.050 V was calculated as before from the applied current and the extrapolated cathodic current (compare to Fig. 1). The anodic current can be approximated by two Tafel lines showing a transition from a low to a high Tafel slope at about +0.05 V. A similar change in the anodic kinetics is also observed at pH 0.00.

In interpreting the change in kinetics with pH, we note that the total potential drop between electrode and solution is given by

$$E = V + \psi_s + (\text{const.}) \qquad (8)$$

Here V is the potential drop across the oxide and ψ_s that across the oxide/electrolyte interface. In view of the large excess of inert electrolyte we may assume in the first approximation that ψ_s does not change with pH. Therefore, for the same $C_{Fe^{+++}}$ and $C_{Fe^{++}}$ or, what is equivalent, at a fixed E_{rev} for the Fe^{+++}/Fe^{++} couple, we have the same V, independent of pH. Since the rate of dissolution increases with acidity, the stationary film thickness must be less in the more acid solutions.

The dissolution rate of passive Ni in 0.5 M $SO_4^=$ is 10^{-7} amp/cm^2 at pH 3.1. Therefore, the direct contribution of ionic current to the total oxidation current is negligible even at low pH. That this is the case is shown by the fact that the rest potential of passive Ni in a Fe^{+3}/Fe^{+2} solution is just the reversible Fe^{+++}/Fe^{++} potential.

The coincidence of the rest potential with the Fe^{+++}/Fe^{++} reversible potential makes it possible to obtain the stoichiometric number for the process from polarization measurements at small current densities. A plot of i vs. (E-Erev) at small (E-Erev) is shown in Fig. 5. The values of $(i_o)_c$ and $(i_o)_a$ given in Table II were obtained from the slope of such plots and the relation

$$\nu = \pm \frac{F}{RT}\, i_o \bigg/ \left(\frac{\partial i}{\partial E}\right)_{(E-Erev)\,=\,0} \qquad (9)$$

The stoichiometric number of a simple one-electron reaction, such as the Fe^{+++}/Fe^{++} reaction, must be unity. Therefore, eq. (9) can be rewritten as

$$i_o = \pm \frac{RT}{F} \left(\frac{\partial i}{\partial E}\right)_{(E-Erev)\,=\,0} \qquad (9a)$$

Consequently, the measurement of $\frac{\partial i}{\partial E}$ at small (E-Erev) provides a check on the exchange currents found by extrapolation from large overpotentials. Specifically, comparison of i_o determined in these two ways shows whether the potential-current relation is the same over the whole of the potential range examined or whether a change in film characteristics takes place as the potential is altered from its equilibrium value.

The results in Table II and Figs. 4 and 5 suggest that the reaction rate and apparent transfer coefficient depend on the thickness of the film and on the pH of the solution in which the film is formed. The increase of the exchange current at low pH is probably caused by changes in film composition which apparently affect its electrochemical characteristics. It has been suggested that protons migrate into surface oxides and are responsible for an increase in conductivity(29, 30). Since the concentration of protons in the film is probably decreased by the additional field imposed on anodic polarization, a more or less continuous increase in the anodic polarization characteristics at low pH is expected as the potential becomes more positive. This is borne out by the low $(i_o)_a$ values calculated from $(\frac{\partial i_a}{\partial E})_{(E-Erev)=0}$ which indicate that the anodic current increases less rapidly at pH of 0.35 and 0.00 than is predicted from the usual expression for the net current at potentials close to equilibrium. The change in the energy of activation for reaction (as calculated from the temperature coefficient of the exchange current, Fig. 6) from 8.5 kcal/mol at pH 2.3 to 4.5 kcal/mol at pH 0.00 also shows that the electrode characteristics are modified substantially by changes of pH.

Iron Electrodes. The passive film on iron is considerably less stable than on nickel. Consequently, high concentrations of ferric ion (0.3 M) were necessary to maintain the electrode in the passive region. Even at this concentration, the rest potential was more active by 10-60 mv than the reversible Fe^{+++}/Fe^{++} potential because of the relatively large corrosion current of passive iron.

The anodic polarization curve on iron electrodes shows hysteresis when overpotential measurements are made relatively rapidly. The time-dependence of the potential suggests that the contribution of the ionic current decreases with time at a fixed anodic current density. An anodic curve was obtained by first polarizing the electrode at 120 $\mu a/cm^2$ until the potential became constant and then rapidly making measurements in decreasing order of current density. In this way, an approximately semilogarithmic polarization curve can be obtained. Measurements under these conditions are shown in Fig. 2.

The polarization curves on passive iron are strongly assymmetrical. The anodic process was examined in detail in M $MgSO_4$ at pH 1.45. The anodic current was held at each value until the potential became constant (~1 mv change in 5 minutes). This required from 10 to 100 minutes, depending on the current. Fig. 7 shows that the anodic current reaches a limiting value which is proportional to the Fe^{++} concentration. This is not a diffusion-limited current. The estimated maximum diffusion currents at the various concentrations used are 10^{-3} to 10^{-2} amp/cm^2, i.e., at least two orders of magnitude greater than the observed limiting currents. Furthermore, comparison with Ni shows that appreciably larger anodic currents can be drawn in that case without any significant contribution from concentration polarization in solution (see Fig. 1).

The i-E characterteristics with passive Fe are analogous to those of a rectifying junction and may be described by an equation formally similar to that applicable to such a junction. Thus, assuming that the current from metal to solution is proportional to the (Fe^{+++}) concentration (as it is with other passive electrodes) we have for the net current in the anodic direction:

$$i_a = k_1 C_{Fe^{++}} - k_2 C_{Fe^{+++}} \exp(-\alpha E)$$

or

$$i_a = k_1 C_{Fe^{++}} \left[1 - \exp(-\alpha E) \right] \qquad (10)$$

where $k_1 C_{Fe^{++}} = k_2 C_{Fe^{+++}}$.

The results with passive Fe are not inconsistent with the general picture of passive films obtained from corrosion studies in the absence of a redox couple in solution$^{(26, 27)}$. For example, Vetter$^{(26)}$ has suggested a model for the passive film in which a potential drop of about

0.6 V is assumed to exist within the oxide. A potential difference across the oxide with no current flowing presupposes a distribution of charge carriers similar to that suggested by the present results.

Titanium Electrodes. Titanium behaves similarly to Fe at temperatures of 30°C and above. Tafel lines are obtained at lower temperatures if the electrode is first anodized at the maximum current density used during a run. Curves similar to those of Fig. 3 are obtained at 0° and 10°C. Curves obtained at 30°C and 40°C are shown in Fig. 8.

The time dependence of the potential (Fig. 9) suggests that the film thickens appreciably on anodic polarization at temperatures above 30°C. At lower temperatures, it is probably unchanged during a cathodic run; it may grow somewhat during an anodic run (see Fig. 9).

The temperature coefficient of the exchange current in the range in which the film thickness was approximately constant yields an energy of activation of about 15 kcal/mol. This is only an estimate, since the $\log i_o$ vs. $1/T$ plots are not straight lines even in this narrow temperature range.

Summary of Polarization Characteristics. The polarization behavior of the Fe^{+++}/Fe^{++} couple on passive Ni, and Ti is given by an expression of the form:

$$i = i_o \left\{ \exp\left[-\alpha_r (E - Erev) \right] - \exp\left[\beta_r (E - Erev - V) \right] \right\} \qquad (11)$$

Here V is the potential drop within the oxide and is, in general, a function of the current density. In general, V is proportional to E, i.e.,

$$V = \gamma E + \text{const.} \qquad (12)$$

In this case,

$$i = i_o \left\{ \exp \left[-\alpha_r \, (E\text{-}Erev) \right] - \exp \left[(\beta_r)(1-\gamma)(E\text{-}Erev) \right] \right\} \qquad (13)$$

Consequently,

$$\alpha_c + \alpha_a = (\alpha_r) + \beta_r (1-\gamma) = 1 - \gamma\beta_r \qquad (14)$$

with an apparent stoichiometric number of:

$$\nu = \pm \frac{F}{RT} \, i_o \Bigg/ \left(\frac{\partial i}{\partial E} \right)_{(E\text{-}Erev) = 0} = 1 - \gamma\beta_r \qquad (15)$$

Equations (12-14) are followed by passive Ni at pH = 2.3 and by Ti at pH = 1.5 and for T ≤ 20°C. The coefficient γ is 0.15 for Ni and 0.60 for Ti. Fe, Ni at low pH, and Ti at higher temperatures show a more complicated behavior on anodic polarization.

Summary and Conclusions.

(1) Passive electrodes generally function as inert, indicator electrodes for the Fe^{+++}/Fe^{++} couple. The ionic current through the passive films of Ni and Ti is negligible compared to electron current. The ionic current is a significant fraction of the total current in the case of passive Fe. The rest potential of passive Fe is a mixed potential and is 10 to 60 mv more negative than the reversible Fe^{+++}/Fe^{++} potential at pH 1.45.

(2) The electrode kinetics of the Fe^{+++}/Fe^{++} reaction on passive electrodes differ substantially from those on oxide-free electrodes, e.g., Pt. The exchange current is substantially smaller on passive electrodes. The anodic transfer coefficient is about the same as on Pt. The sum of the apparent anodic and cathodic transfer coefficients on passive electrodes is significantly less than unity.

(3) The i-E characteristics of the metal/passive film/redox electrolyte system are asymmetrical. The direction of easy electron flow is

from metal to solution. A limiting anodic current, which is unrelated to diffusion of Fe^{++} in solution, is observed on Fe and Ti in certain cases.

(4) The polarization characteristics of the Fe^{+++}/Fe^{++} reaction on passive Ni, Fe, and Ti, specifically the unusual behavior summarized in (2) and (3), suggest that a potential drop exists within the oxide and that this potential is particularly important in anodic polarization. This conclusion is consistent with other studies of the growth and dissolution of passive films.

REFERENCES

1 M. Breiter in "Advances in Electrochemistry and Electrochemical Engineering", Vol. I, p. 123, John Wiley & Sons, New York, 1961

2 K. F. Bonhoeffer and K. J. Vetter, Z. phys. Chem., 196, 127 (1951)

3 K. J. Vetter, Z. Elektrochem., 58, 230 (1954); 59, 67 (1955)

4 U. F. Franck and K. G. Weil, Z. Elektrochem., 56, 814 (1952)

5 K.G. Weil, Z. Elektrochem., 59, 711 (1955)

6 Y. M. Kolotyrkin, Z. Elektrochem., 62, 664 (1958)

7 H. Gerischer, Z. Elektrochem., 54, 362 (1950)

8 J.E.B. Randles and K.W. Somerton, Trans. Faraday Soc., 48, 937 (1952)

9 A. C. Makrides, J. Electrochem. Soc., 109, 977 (1962)

10 M. Stern and A. C. Makrides, J. Electrochem. Soc., 107, 782 (1960)

11 C. V. King and L. Weidenhammer, J. Am. Chem. Soc., 58, 602 (1936); A. C. Makrides and N. Hackerman, J. Electrochem. Soc., 105, 156 (1958)

12 C. V. King, J. Electrochem. Soc., 102, 193 (1955)

13 M. Stern, J. Electrochem. Soc., 104, 559, 600 (1957)

14 F. A. Posey, J. Electrochem. Soc., 106, 582 (1959)

15 T. Ishikawa and G. Okamoto, First Intl. Congress Met. Corrosion, 1961, Butterworths, London, p. 104

16 R. E. Meyer, J. Electrochem. Soc., 107, 847 (1960)

17 R. W. Gurney, Proc. Royal Soc. (London), A134, 137 (1931)

18 R. A. Marcus, J. Chem. Phys., 24, 966(1956); also in "Electrode Processes", John Wiley, New York, 1961, p. 239

19 H. Gerischer, Z. phys. Chem., N.F., 26, 223, 325 (1960); 27, 48 (1961)

20 A. Charlesby, Acta Met., 1, 348 (1953)

21 D. A. Vermilya, Acta Met., 2, 346 (1954)

22 A. W. Smith, Can. J. Phys., 35, 1151 (1957)

23 W. Ch. van Geel and J. W. A. Scholte, Philips Res. Rept., 6, 54 (1951); J. W. A. Scholte and W. Ch. van Geel, ibid, 8, 47 (1953)

24 H. E. Haring, J. Electrochem. Soc., 99, 30 (1952)

25 D. A. Vermilya, J. Appl. Phys., 27, 963 (1956)

26 K. J. Vetter, Z. Elektrochem., 62, 642 (1958)

27 M. Nagayama and M. Cohen, J. Electrochem. Soc., 109, 781 (1962)

28 N. Sato and G. Okamoto, Trans. Jap. Inst. Metals, 2, 113 (1961)

29 P. F. Schmidt, J. Appl. Phys., 28, 278 (1957)

30 P. D. Lukovtsev and G. J. Slaidin, Acta Electrochim. 6, 17 (1962)

TABLE I

Overpotential Parameters for the Fe^{+++}/Fe^{++} Couple

$C_{Fe^{+++}} = C_{Fe^{++}} = 0.05$ M

Electrode	H_2SO_4	T(°C)	i_o(amp/cm^2)	α_c	α_a	$\alpha_c + \alpha_a$
Ni	M/100$^{(1)}$	30°	7.5×10^{-5}	0.41	0.49	0.90
Fe	M/20$^{(2)}$	40°	(1×10^{-5})	0.69	(0.23)	(0.92)
Ti	M/20$^{(1)}$	20°	2.6×10^{-7}	0.47_5	0.16_5	0.64
Pt$^{(3)}$	M	25°	1.5×10^{-2}	0.42	0.58	1.00

---

(1) Solution M in $MgSO_4$.

(2) Solution M/10 in Na_2SO_4.

(3) Results of Gerischer, ref. 7.

TABLE II

Nickel (1)

pH	$T(^{o}C)$	$E_{corr}(v)$	i_o extrapolated from cathodic curve (amp/cm^2)	i_o from $\frac{(\partial i)}{(\partial E)}_{(E-Erev)=0}$		α_c	α_a	$\alpha_c+\alpha_a$
				$(i_o)_c$	$(i_o)_a$			
2. 3	10^{o}	-0. 0003	2.6×10^{-5}	2.5×10^{-5}	2.5×10^{-5}	0. 415	0. 484	0. 90
	20^{o}	-0. 0006	4.55×10^{-5}	4.4×10^{-5}	4.4×10^{-5}	0. 40	0. 495	0. 90
	30^{o}	-0. 0012	7.6×10^{-5}	7.45×10^{-5}	7.15×10^{-5}	0. 41	0. 49	0. 90
0. 35	30^{o}	-0. 0006	8.6×10^{-5}	8.6×10^{-5}	7.5×10^{-5}	0. 46	(0. 60) (0. 375)	--
0. 00	0^{o}	-0. 0003	5.0×10^{-5}	--	--	0. 47	--	--
	10^{o}	-0. 0008	8.0×10^{-5}	--	--	0. 47	--	--
	20^{o}	-0. 0005	$11. \times 10^{-5}$	10.2×10^{-5}	8.0×10^{-5}	0. 47	--	--
	30^{o}	-0. 001	$14. \times 10^{-5}$	12.8×10^{-5}	7.0×10^{-5}	0. 47	(0. 33)	--

---

(1) All solutions $C_{Fe^{+++}} = C_{Fe^{++}} = 0.050M$ and M $MgSO_4$.

FIGURE CAPTIONS

Fig. 1 Polarization curves for the Fe^{+++}/Fe^{++} couple (0.05 M) on Ni electrodes in M $MgSO_4$ at pH = 2.3 and at 30°C. Current densities corresponding to the full circles are calculated from $i_{ox} = i_{appl} + i_{red}$ where i_{red} is given by the extrapolated cathodic curve.

Fig. 2 Polarization curves for the Fe^{+++}/Fe^{++} couple (0.05 M) on Ti electrodes in M $MgSO_4$ at pH = 2.3 and at 20°C. Current densities corresponding to the full circles are calculated from $i_{ox} = i_{appl} + i_{red}$ where i_{red} is given by the extrapolated cathodic curve.

Fig. 3 Polarization curves for the Fe^{+++}/Fe^{++} couple on Fe electrodes at 40°C. The solution was 0.30 M in Fe^{+++}, 0.03 M in Fe^{++}, and M/20 in H_2SO_4 and M/10 in Na_2SO_4. The anodic curve was obtained after the electrode was kept for 30 min. at 0.20 V vs. Erev for Fe^{+++}/Fe^{++}.

Fig. 4 Polarization curves for the Fe^{+++}/Fe^{++} couple (0.05 M) on Ni electrodes in M $MgSO_4$ at pH = 0.35 and at 30°C. Current densities corresponding to the open circles are calculated from $i_{ox} = i_{appl} + i_{red}$ where i_{red} is given by the extrapolated cathodic curve.

Fig. 5 Linear plots of (E - Erev) vs. current density for the Fe^{+++}/Fe^{++} couple (0.05 M) on Ni electrodes in M $MgSO_4$ at pH = 0.35 and at 30°C. The apparent stoichiometric number, determined from the cathodic polarization curve, is unity.

Fig. 6 Arrhenius plots for the Fe^{+++}/Fe^{++} couple (0.05 M) on Ni electrodes in M $MgSO_4$. The exchange current, i_o, is that extrapolated from the cathodic curve. The activation energies are 8.5 kcal at pH = 2.3 and 4.5 kcal at pH = 0.0.

Fig. 7 Anodic polarization curves for the Fe^{+++}/Fe^{++} couple on iron in M $MgSO_4$ at pH = 1.45. The Fe^{+++} concentration was 0.3 M. The current was kept constant at each value shown until the potential changed by less than 1 mv in 5 min.

Fig. 8 Polarization curves for the Fe^{+++}/Fe^{++} couple (0.05 M) on Ti electrodes in M $MgSO_4$ at pH = 2.3.

Fig. 9 Time dependence of the potential of Ti electrodes in a Fe^{+++}/Fe^{++} (0.05 M) solution. M in $MgSO_4$ and of pH = 2.3. The applied anodic current densities are given in the Figure together with the temperature for each measurement.

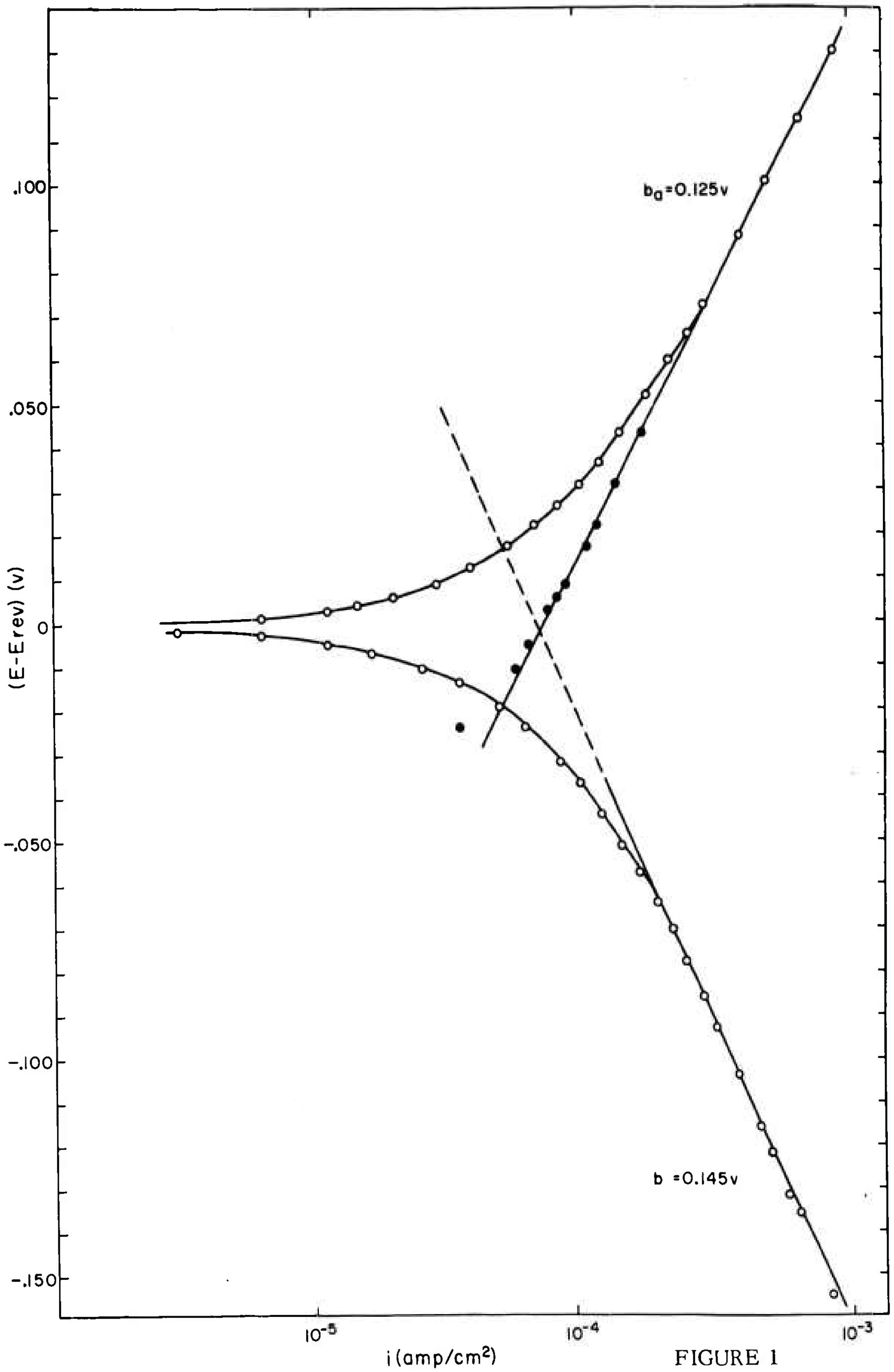

.100
.050
0
-.050
-.100
-.150
(E-Erev) (v)
10^{-5}
10^{-4}
10^{-3}
i (amp/cm²)
b_a=0.125v
b =0.145v

FIGURE 1

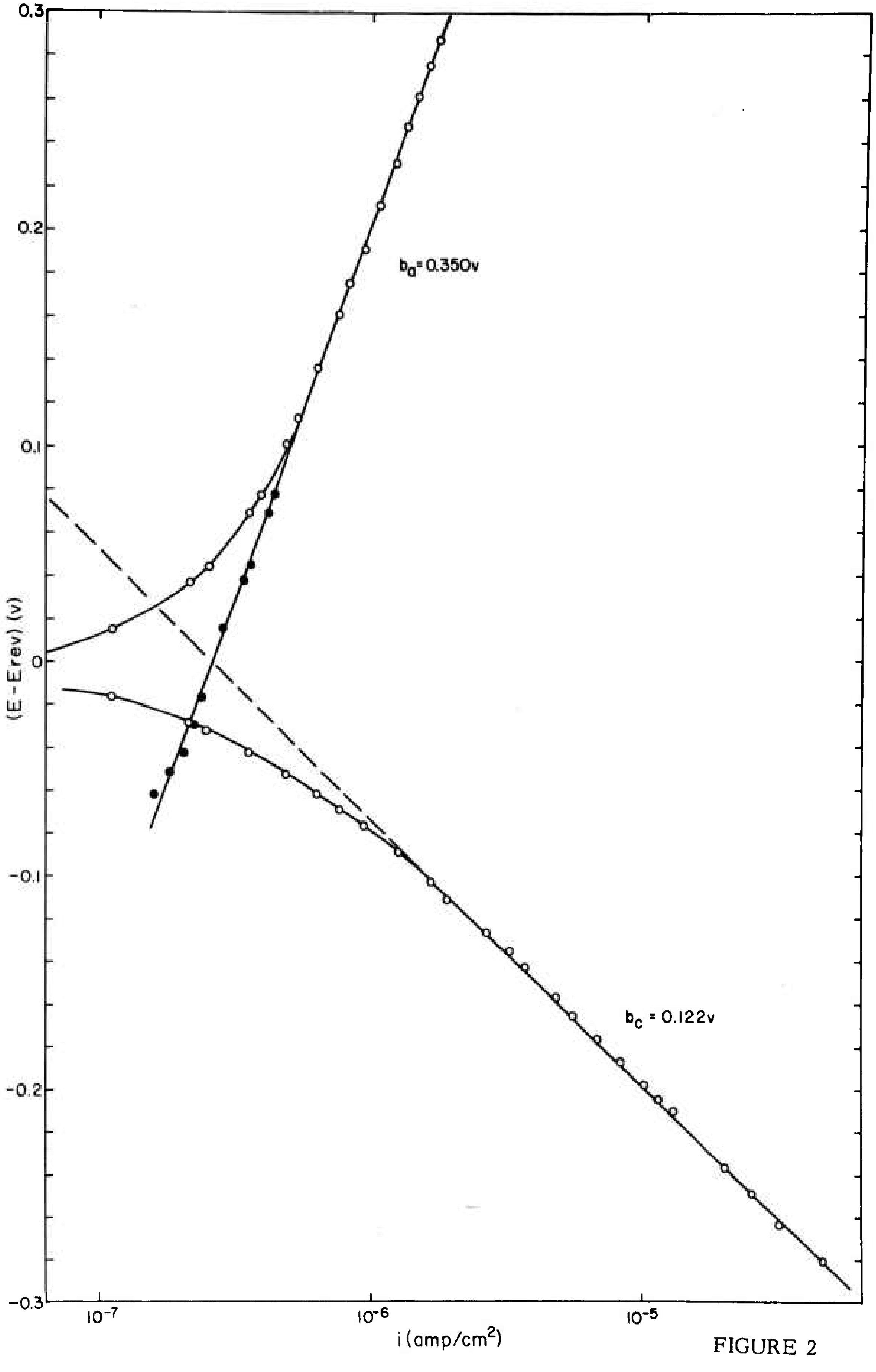

FIGURE 2

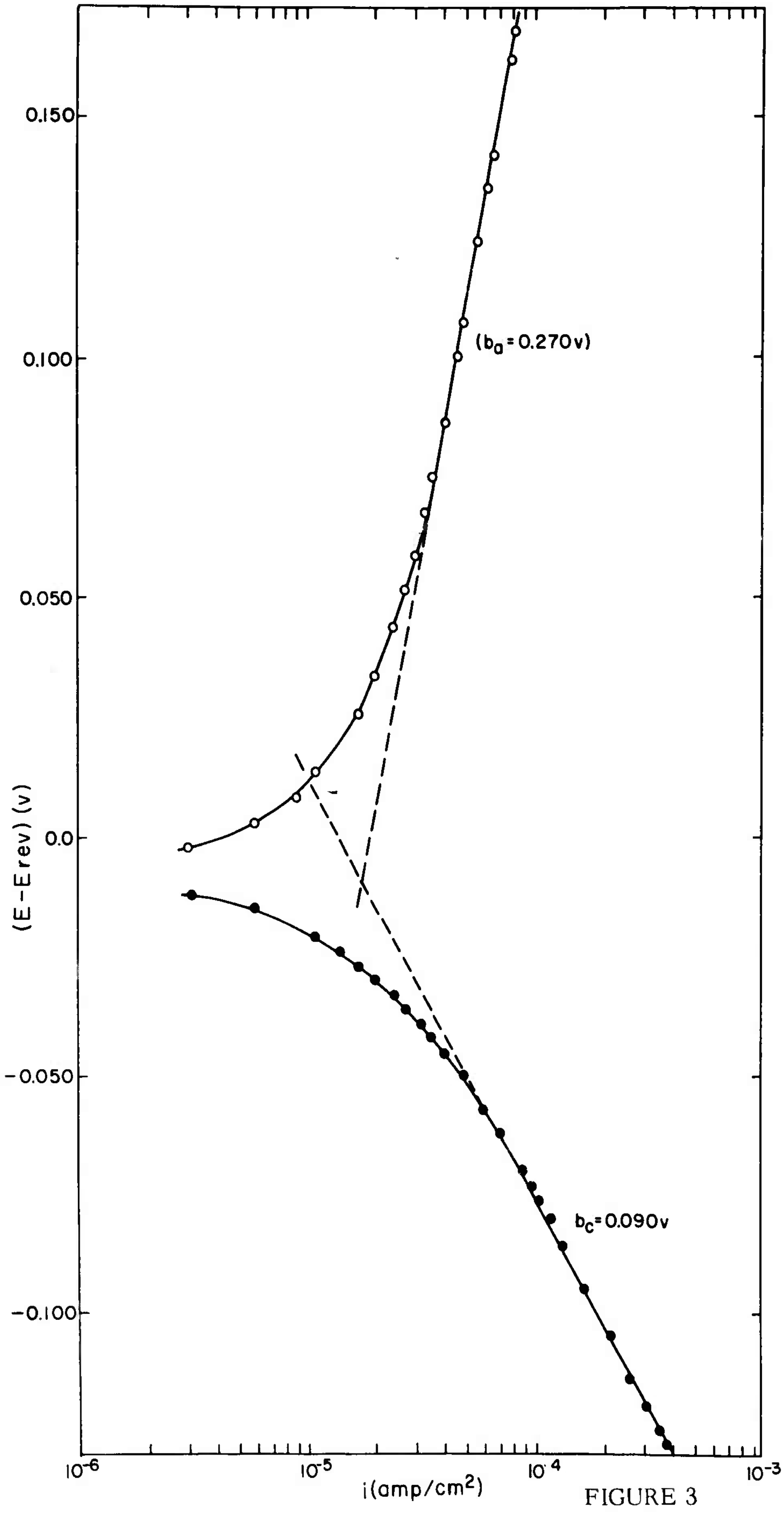
0.150
0.100
0.050
0.0
-0.050
-0.100
(E-Erev) (v)
10^{-6}
10^{-5}
10^{-4}
10^{-3}
i(amp/cm^2)
(b_a=0.270v)
b_c=0.090v

FIGURE 3

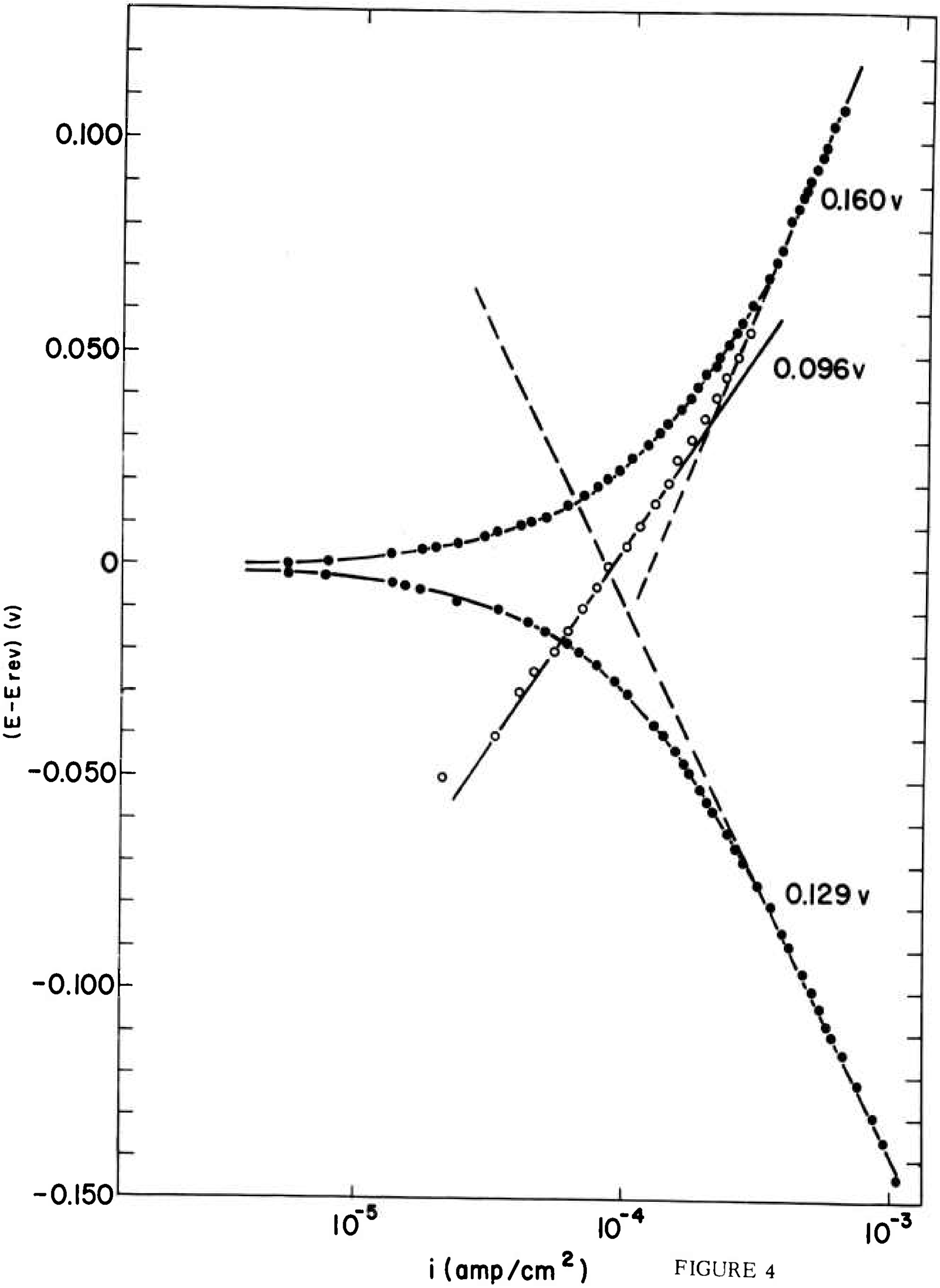
0.100
0.050
0
-0.050
-0.100
-0.150
(E-E rev) (v)
10^{-5}
10^{-4}
10^{-3}
i (amp/cm^2)
0.160 v
0.096 v
0.129 v

FIGURE 4

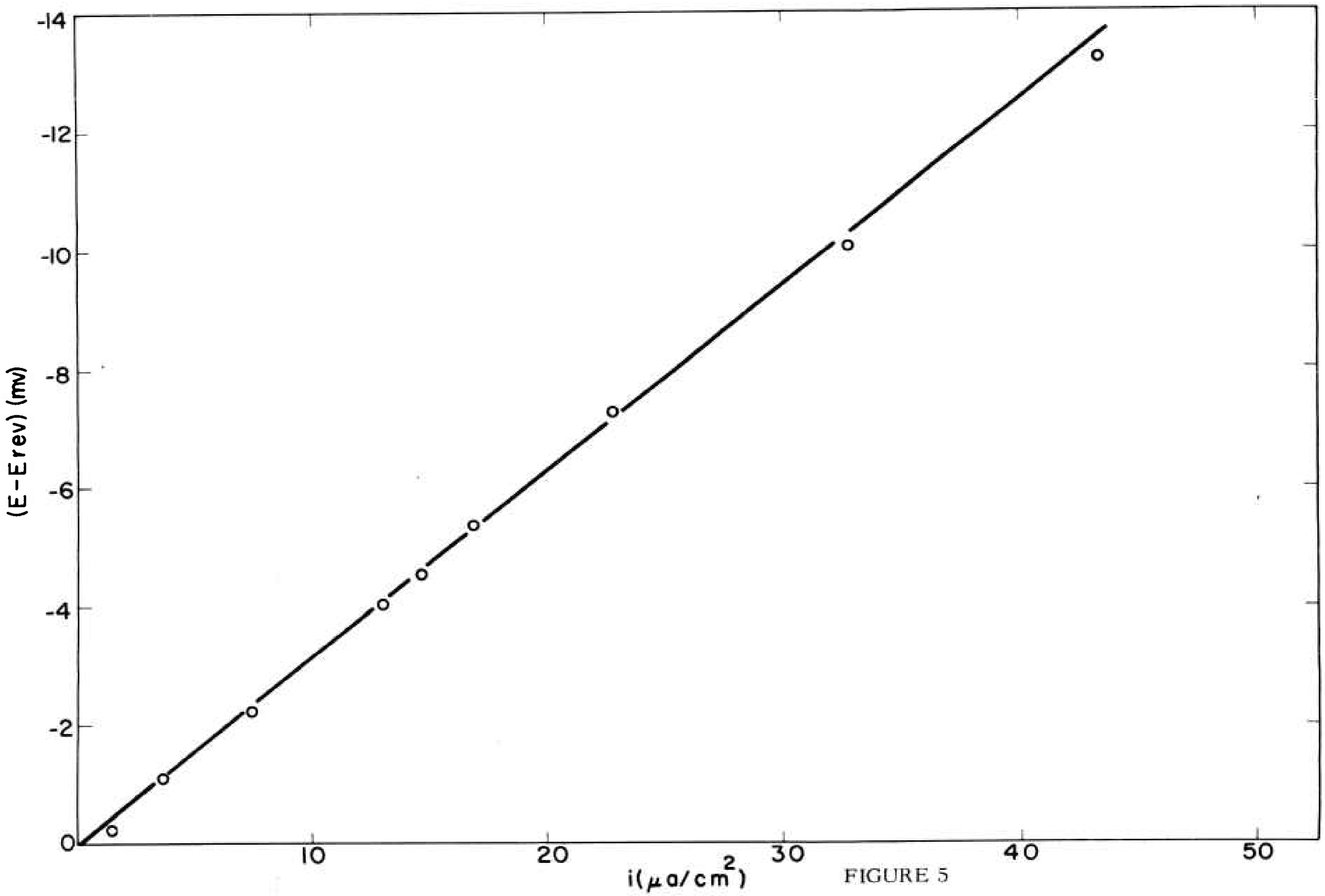

FIGURE 5

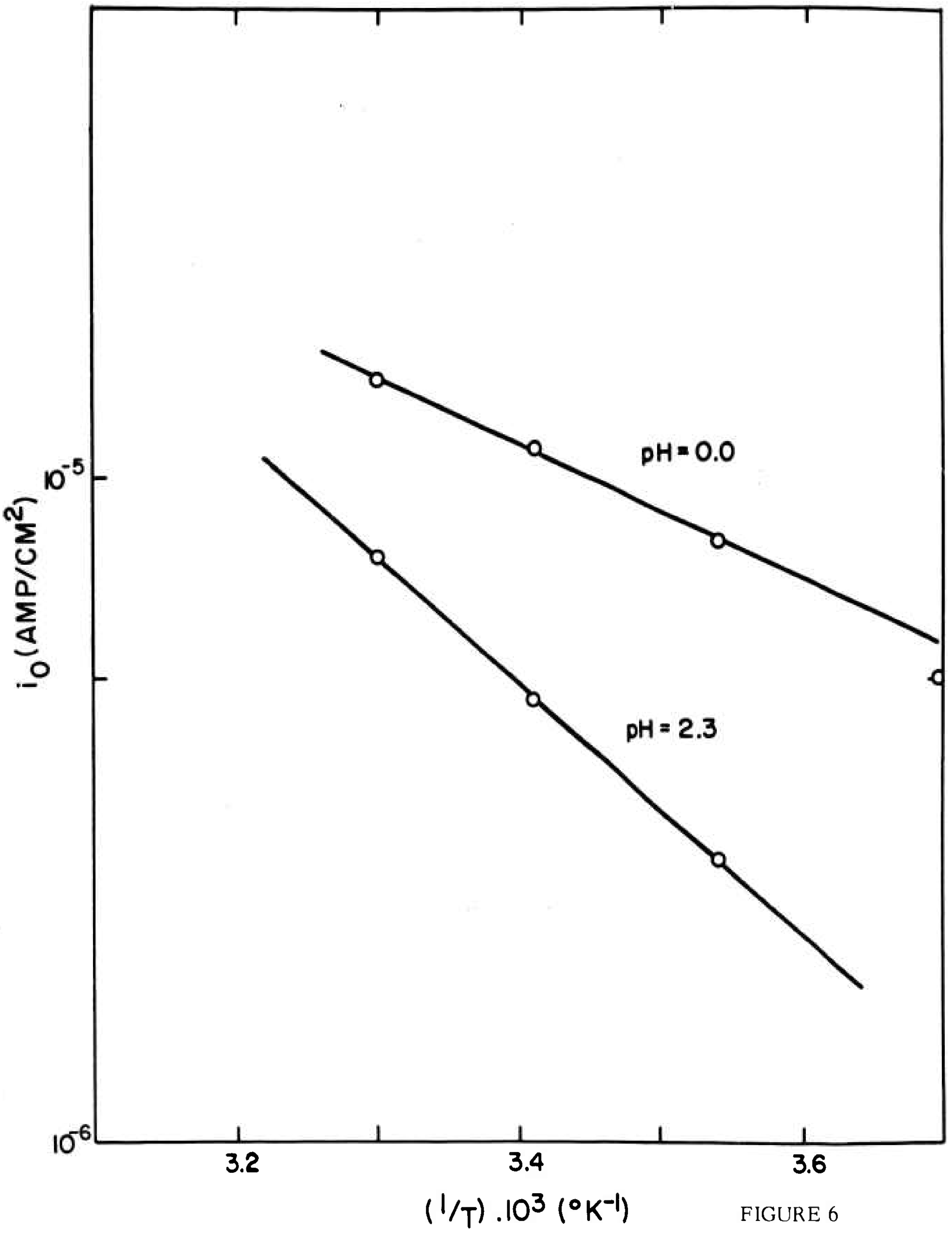

FIGURE 6

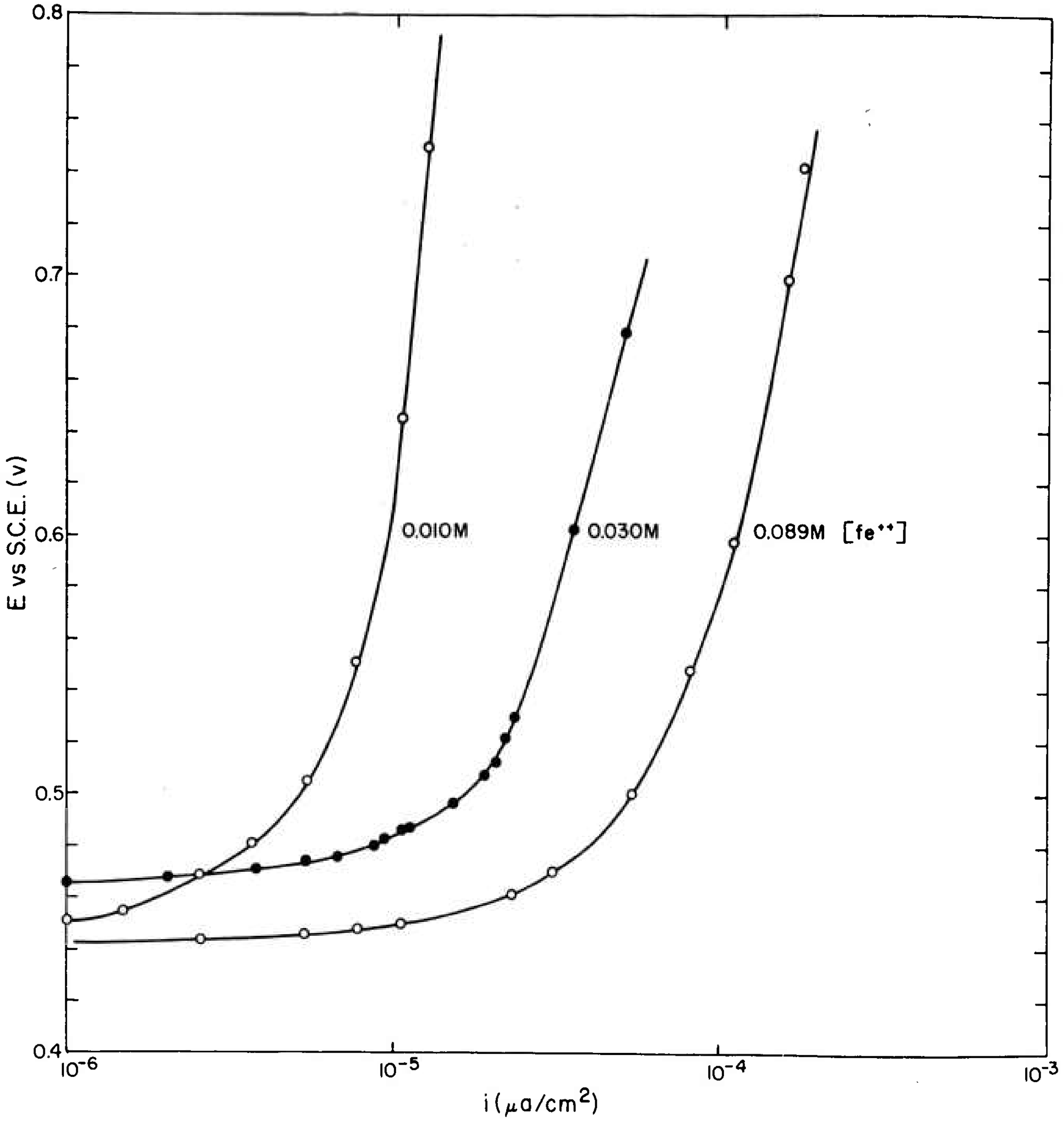
0.8
0.7
0.6
0.5
0.4
E vs S.C.E. (v)
0.010M
0.030M
0.089M [fe⁺⁺]
10⁻⁶
10⁻⁵
10⁻⁴
10⁻³
i (μa/cm²)

FIGURE 7

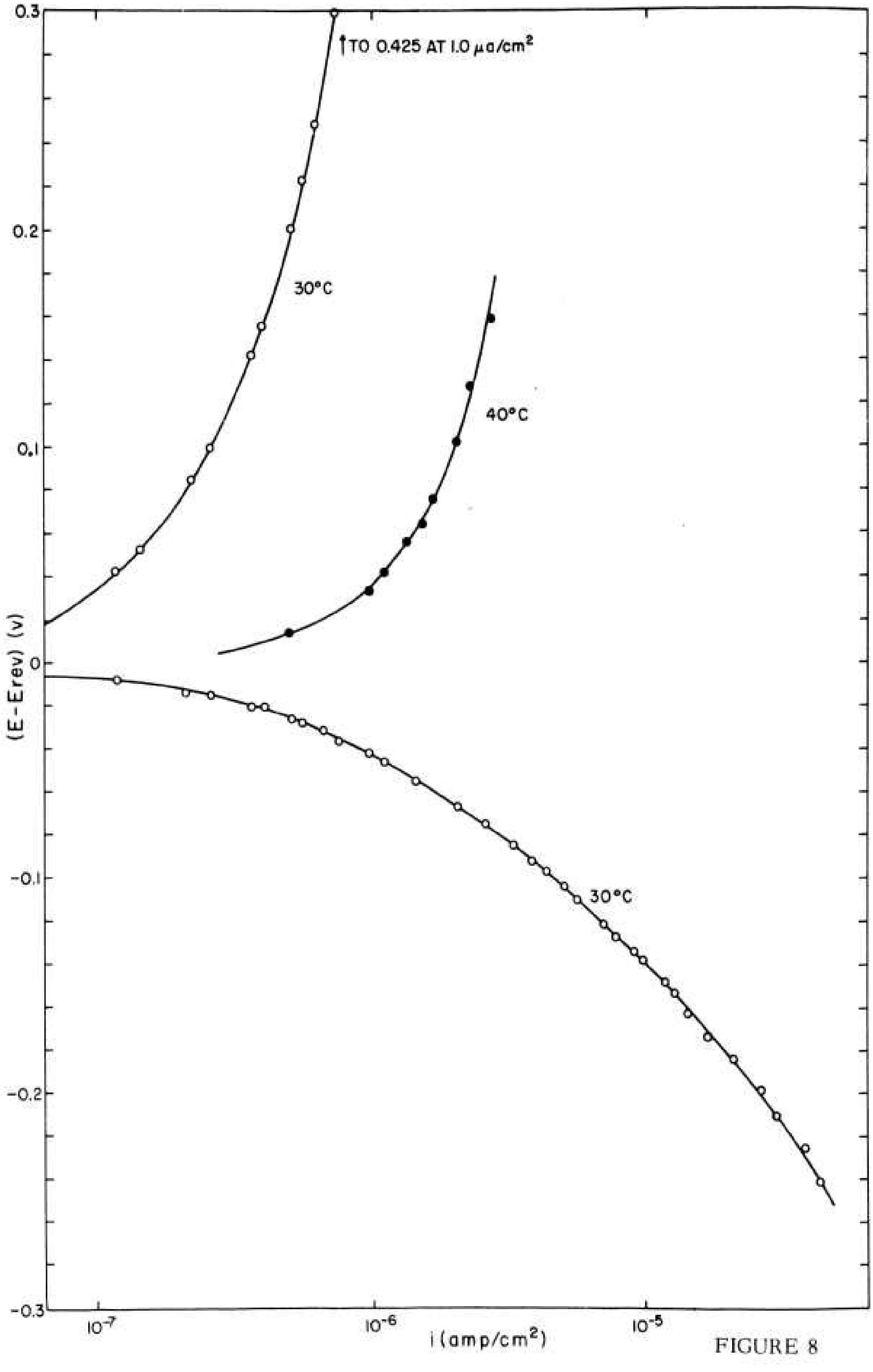
↑TO 0.425 AT 1.0 μa/cm²
30°C
40°C
30°C
0.3
0.2
0.1
0
-0.1
-0.2
-0.3
(E-Erev) (v)
10⁻⁷
10⁻⁶
10⁻⁵
i (amp/cm²)

FIGURE 8

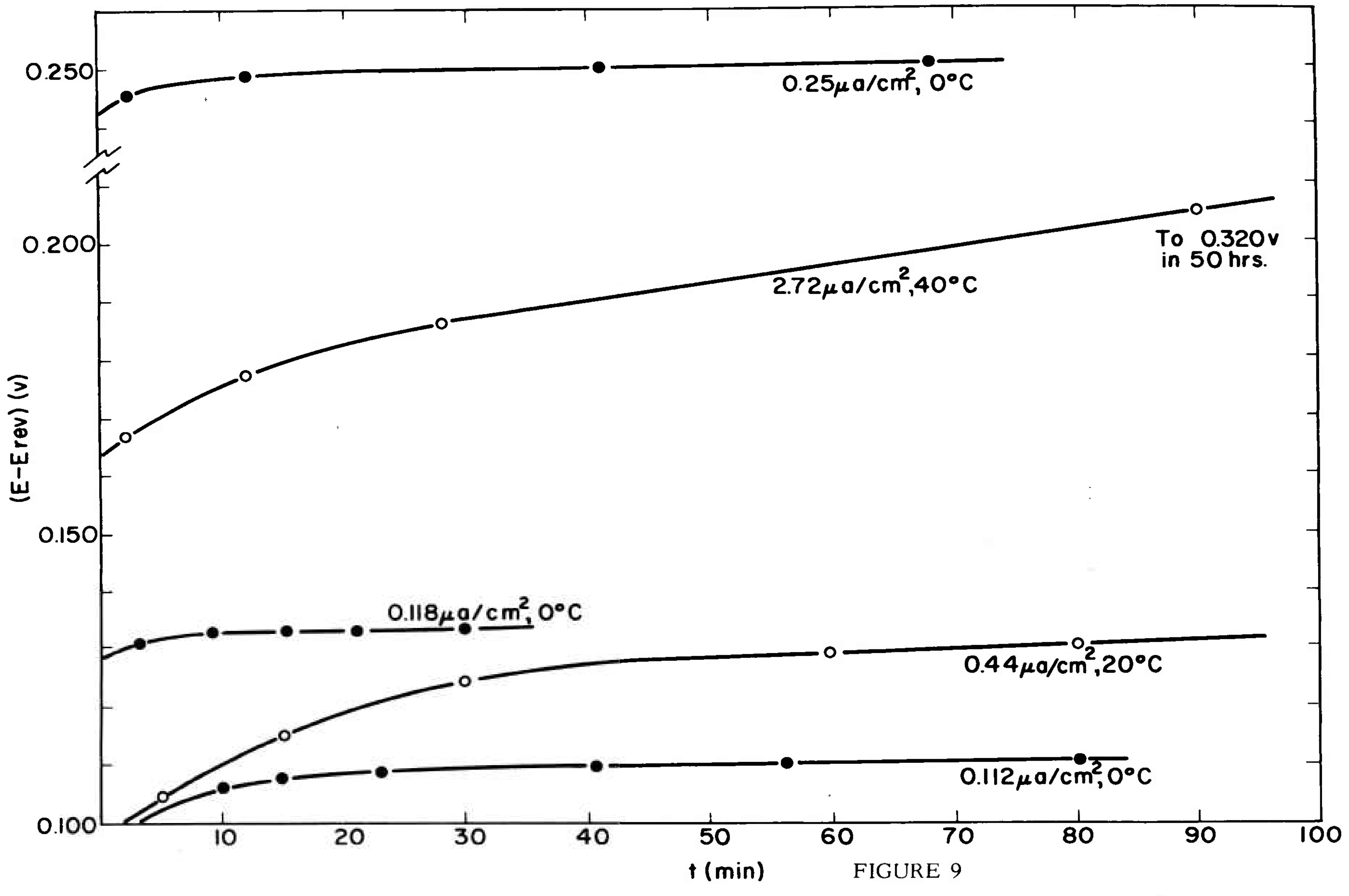
0.250
0.200
0.150
0.100
(E−Erev) (v)
0.25μa/cm², 0°C
2.72μa/cm²,40°C
To 0.320v
in 50 hrs.
0.118μa/cm², 0°C
0.44μa/cm²,20°C
0.112μa/cm², 0°C
10
20
30
40
50
60
70
80
90
100
t (min)

FIGURE 9

TECHNICAL REPORT DISTRIBUTION LIST

Contract No. Nonr 3765(00)

Commanding Officer
Office of Naval Research Branch Office
The John Crerar Library Building
86 East Randolph Street
Chicago 1, Illinois (1)

Commanding Officer
Office of Naval Research Branch Office
346 Broadway
New York 13, New York (1)

Commanding Officer
Office of Naval Research Branch Office
1030 East Green Street
Pasadena 1, California (1)

Commanding Officer
Office of Naval Research Branch Office
Box 39 Navy #100 Fleet Post Office
New York, New York (7)

Director, Naval Research Laboratory
Washington 25, D.C.
Attn: Technical Information Officer (6)
Chemistry Division (2)

Chief of Naval Research
Department of the Navy
Washington 25, D.C.
Attn. Code 425 (2)

DDR&E
Technical Library
Room 3C-128, The Pentagon
Washington 25, D.C. (1)

Technical Director
Research & Engineering Division
Office of the Quartermaster General
Department of the Army
Washington 25, D.C. (1)

Research Director
Clothing & Organic Materials Division
Quartermaster Research & Engineering
Command, U.S. Army
Natick, Massachusetts (1)

Air Force
Office of Scientific Research (SRC-E)
Washington 25, D.C. (1)

Commanding Officer
Diamond Ordnance Fuze Labs.
Washington 25, D. C.
Attn: Technical Information Office
Branch 012 (1)

Office, Chief of Research &
Development, Dept. of the Army
Washington 25, D.C.
Attn: Physical Sciences Div. (1)

Chief, Bureau of Ships
Department of the Navy
Washington 25, D.C.
Attn: Code 342C (2)

Chief, Bureau of Naval Weapons
Department of the Navy
Washington 25, D.C.
Attn: Technical Library (4)

ASTIA
Document Service Center
Arlington Hall Station
Arlington 12, Virginia (10)

Director of Research
U.S. Army Signal Research &
Development Laboratory
Fort Monmouth, New Jersey (1)

Naval Radiological Defense
Laboratory
San Francisco 24, California
Attn: Technical Library (1)

Naval Ordnance Test Station
China Lake, California
Attn: Head,
Chemistry Division (1)

Commanding Officer
Army Research Office
Box CM, Duke Station
Durham, North Carolina
Attn: Scientific Synthesis Office (1)

Brookhaven National Laboratory
Chemistry Department
Upton, New York (1)

Atomic Energy Commission
Division of Research
Chemistry Programs
Washington 25, D.C. (1)

Atomic Energy Commission
Division of Technical Information Extension
Post Office Box 62
Oak Ridge, Tennessee (1)

U.S. Army Chemical Research and Development Laboratories
Technical Library
Army Chemical Center, Maryland (1)

Office of Technical Services
Department of Commerce
Washington 25, D.C. (1)

Commanding Officer
Office of Naval Research Branch Office
495 Summer Street
Boston 10, Massachusetts (1)

Director, ARPA
Attn: Dr. J. H. Huth
Material Sciences
Room 3D155 The Pentagon
Washington 25, D.C. (4)

Dr. S. Schuldiner
Naval Research Laboratory
Code 6160
Washington 25, D. C. (1)

Dr. R.F. Baddour
Department of Chemistry
Mass. Institute of Technology
Cambridge 39, Massachusetts (1)

Inspector of Naval Material
495 Summer Street
Boston 10, Massachusetts (1)

Mr. R.A. Osteryoung
Atomics International
Canuga Park, California (1)

Dr. David M. Mason
Stanford University
Stanford, California (1)

Dr. Howard L. Recht
Astropower, Inc.
2968 Randolph Avenue
Costa Mesa, California (1)

Mr. L.R. Griffith
California Research Corporation
576 Standard Avenue
Richmond, California (1)

Dr. Ralph G. Gentile
Monsanto Research Corporation
Boston Laboratories
Everett 49, Massachusetts (1)

Mr. Ray M. Hurd
Texas Research Associates
1701 Guadalupe Street
Austin 1, Texas (1)

Dr. C. E. Heath
Esso Research & Engineering Company
Box 51
Linden, New Jersey (1)

Dr. Richard H. Leet
American Oil Company
Whiting Laboratories
Post Office Box 431
Whiting, Indiana (1)

Dr. G. C. Szego
Institute for Defense Analysis
1666 Connecticut Avenue N.W.
Washington 9, D.C. (1)

Dr. Douglas W. McKee
General Electric Company
Research Laboratories
Schenectady, New York (1)

Dr. E. A. Oster
General Electric Company, DECO
Lynn, Massachusetts (1)

Dr. R.R. Heikes
Solid State Phenomena Department
Westinghouse Electric Corporation
Pittsburgh, Pennsylvania

Prof. Herman P. Meissner
Massachusetts Institute of Technology
Cambridge 39, Massachusetts (1)

Mr. Donald P. Snowden
General Atomic
Post Office Box 608
San Diego 12, California (1)

Mr. C. Tobias
Chemistry Department
University of California
Berkeley, California (1)

Mr. Y. L. Sandler
Westinghouse Research Laboratories
Schenectady, New York (1)

Dr. Paul Delahay
Department of Chemistry
Louisiana State University
Baton Rouge, Louisiana (1)

Dr. W. J. Hamer
Electrochemistry Section
National Science Foundation
Washington 25, D. C. (1)

Dr. Herbert Hunger
Power Sources Division
U. S. Army Signal Research &
Development Laboratory
Fort Monmouth, New Jersey

Dr. T.P. Dirkse
Department of Chemistry
Calvin College
Grand Rapids, Michigan (1)

Dr. George J. Janz
Department of Chemistry
Rensselaer Polytechnic Institute
Troy, New York (1)

Mr. N. F. Blackburn
E. R. D. L.
Materials Branch
Fort Belvoir, Virginia (1)

Dr. G. Barth-Wehrenalp, Director
Inorganic Research Department
Pennsalt Chemicals Corporation
Box 4388
Philadelphia 18, Pennsylvania (2)

Dr. B. R. Sundheim
Department of Chemistry
New York University
New York 3, New York (1)

Dr. B. R. Stein
European Research Office
U. S. Army R&D Liaison
Group 985 IDU
APO 757, New York, N. Y. (1)

Dr. E. M. Cohn
NASA
Code RPP
1512 H Street N. W.
Washington 25, D. C. (1)

Dr. E. Yeager
Department of Chemistry
Western Reserve University
Cleveland 6, Ohio (1)

Lockheed Aircraft Corporation
Missiles and Space Division
Technical Information Center
3251 Hanover Street
Palo Alto, California (1)